

Amplification of noise in a cascade chemical reaction

Tatsuo Shibata*

*Abteilung Physikalische Chemie, Fritz-Haber-Institut der Max-Planck-Gesellschaft, Faradayweg 4-6, 14195 Berlin (Dahlem), Germany
and Department of Mathematical and Life Sciences, University of Hiroshima, 1-3-1, Kagamiyama, Higashi-Hiroshima,
739-8526, Japan*

(Received 22 December 2003; published 24 May 2004)

Networks of chemical reactions have been given much attention recently. However, dynamical aspects of such networks remain to be elucidated. In this paper, we study a cascade chemical reaction, consisting of a series of downstream-coupled Brusselators. Along the cascade of reaction, small fluctuations naturally existing in the concentration of chemical species are amplified. Such amplification of small noise leads to the formation of chemical oscillations in the downstream chemical species. The amplification rate of small noise in the concentration along the cascade is studied and the method to calculate the amplification rate analytically is developed. It is also shown that the nonlinear evolution of the chemical oscillation in the downstream reaction strongly depends on the frequency of the initial inlet chemical concentration.

DOI: 10.1103/PhysRevE.69.056218

PACS number(s): 05.45.-a, 82.40.Qt, 47.27.Te

I. INTRODUCTION

In flow systems with *convective instability*, small disturbances are amplified as they are advected downstream. Examples of such flow systems have been found in fluid dynamics and nonlinear optics [1–3]. The nonlinear evolution of small disturbances in these systems results in the formation of wave patterns and spatiotemporal chaotic motions. In the system with convective instability, the amplification of disturbances is observed only in a co-moving frame, while the disturbances themselves are damped in time. Therefore, such amplification and formation of patterns are said to be *noise sustained*. The formation of patterns is typically sensitive to the frequency of the upstream small amplitude modulation.

The basic mechanism underlying such phenomena has been explored theoretically for relatively simple dynamical systems. Distributed dynamical systems with unidirectional coupling are among them. They have been shown to exhibit amplification of small disturbances along the unidirectional coupling, similar to flow systems. For these systems, concepts available in flow systems have been developed such as the co-moving Lyapunov exponent [4,5,7] and a pattern formation that is sensitive to the frequency of boundary modulation [2,6].

Such a flow system could also be found in a cascade of chemical reactions or reaction networks [11], where a flux of reactions propagates along the series of successive chemical reactions. Chemical plant could be an example of them. Biological systems could also provide a variety of examples of such flow systems [12]. Cascades of chemical reactions in cells are found in signal transduction and gene regulatory networks. Frequency-sensitive cellular response has been observed experimentally [13]. Amplification of stimuli information is one of the important properties of cellular signal transduction. Since chemical reaction is a stochastic process, the concentrations of molecular species inevitably fluctuates

in time. Thus, if the reaction network is “convectively unstable” along the reaction cascades, a noise-sustained structure could arise, even without spatial coordinates. In particular, the noise-sustained formation of patterns in a small reaction system such as cells could be interesting.

In the present paper, we first consider a model of a cascade chemical reaction and demonstrate that the system shows convective instability. Although the cascade chemical reaction has no spatial coordinate, small disturbances in the inlet chemical concentration are amplified along the cascade. Then, the problem which we want to address in this publication is how to determine the rate of the amplification of small disturbances along the cascade chemical reaction.

For the characterization of the convective unstable spatial extended systems, the co-moving Lyapunov exponent, which is the growth rate of small disturbances in a moving frame, has been widely used [4]. If the maximum co-moving Lyapunov exponent is positive while the Lyapunov exponent is negative, small noise applied at the inlet is amplified and the noise sustains formation of patterns. Such noise-sustained amplification can be characterized by the spatial Lyapunov exponent [8,9]. The spatial Lyapunov exponent is the amplification rate of the noise strength along the spatial coordinate. The spatial Lyapunov exponent can be calculated according to the relation between the co-moving and its velocity [8,9].

In this paper, the spatial Lyapunov exponent is calculated explicitly by applying the Fourier analysis, and the results are then compared with the previous method using the co-moving Lyapunov exponent. Since the concept of the spatial Lyapunov exponent is applicable to systems without spatial coordinate, here we call it the “amplification exponent.” This analysis also gives the frequency-dependent amplification exponent. Then, we discuss the pattern selection by modulating the input chemical concentration.

This paper is organized as follows. The cascade chemical reaction model is proposed in Sec. II, and the amplification of small perturbations and the formation of chemical oscillation are described. In Sec. III, the convective instability is characterized by the co-moving Lyapunov exponent. In Sec.

*Electronic address: shibata@hiroshima-u.ac.jp

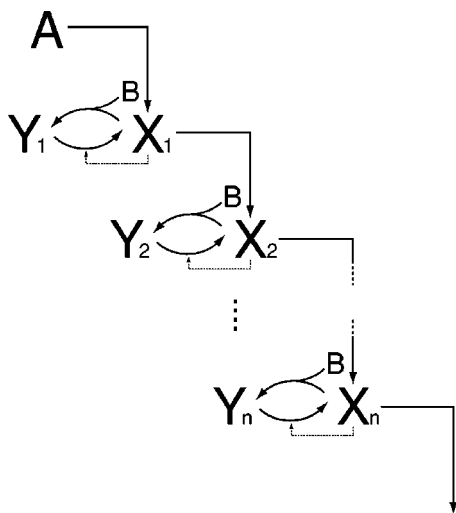
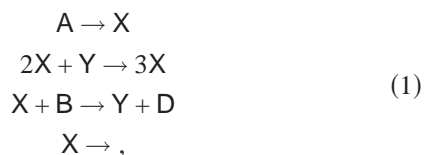


FIG. 1. The cascade Brusselator. The first step chemical reaction for chemical species X_1 and Y_1 is Brusselator. In the n th step, chemical reactions among X_n and Y_n occur according to Brusselator, except X_n is synthesized from X_{n-1} but not from A.

IV, the amplification rate of small disturbances is calculated analytically and then compared with the amplification rate obtained numerically from the co-moving Lyapunov exponent. In Sec. V, the effect of modulating the inlet chemical concentration is studied. Discussion and conclusions are given in Sec. VI.

II. CASCADE BRUSSELATOR

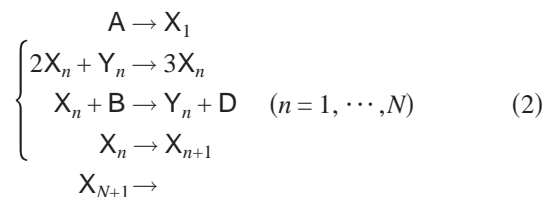
We start with the well understood nonlinear chemical reaction, the Brusselator, which is given by



where, A, B, and D are the chemical species with constant concentrations, whereas the concentration of chemical species X and Y can change in time.

In order to construct a model cascade reaction, consider a series of such Brusselators. The first chemical reaction for chemical species X_1 and Y_1 is the Brusselator, given by scheme 1. The next chemical reaction for the chemical species X_2 and Y_2 is also a Brusselator, but X_2 is synthesized from X_1 , instead of A. The n th reaction for X_n and Y_n is also a Brusselator, and X_n is synthesized from X_{n-1} (see Fig. 1). In this way, we consider the chemical reactions among

chemical species $\{X_1, X_2, \dots, X_N\}$ and $\{Y_1, Y_2, \dots, Y_N\}$, which is given by



Let x_n and y_n represent the concentrations of the chemical species X_n and Y_n , ($n = 1, 2, \dots, N$) and a and b be the concentrations of the input chemical species A and B, respectively. Then, the macroscopic evolution equations for the concentration of X_n and Y_n are given by

$$\begin{aligned}
 \dot{x}_n &= x_{n-1} + x_n^2 y_n - b x_n - x_n \quad (n = 1, \dots, N), \\
 \dot{y}_n &= -x_n^2 y_n + b x_n
 \end{aligned}
 \quad (3)$$

with $x_0 = a$.

The fixed point of this system is given by $(x_n^*, y_n^*) = (a, b/a)$. This fixed point (x^*, y^*) is stable if the condition $b < a^2 + 1$ is satisfied and is unstable if $b > a^2 + 1$. This stability condition is the same as that of the single Brusselator. If $b > a^2 + 1$ and hence the fixed point is unstable, the limit cycle emerges in each component and the phase of the oscillation propagates from the first reaction to downstream reactions.

If no disturbances exist, except for the perturbations of initial conditions, and the above stability condition is satisfied, the perturbations of initial conditions are damped out and the concentrations approach to the fixed point. In this case the Lyapunov exponent is negative. However, even when the system satisfies the stability conditions and hence the Lyapunov exponent is negative, if some disturbances exist at the top of the reaction step, such a disturbance can grow in the downstream reactions. For instance, consider the case where the concentration of A fluctuates in time. Then the evolution equation is given by Eq. (3) with

$$x_0(t) = a + \eta(t), \quad (4)$$

where $\eta(t)$ is the Gaussian white noise with $\langle \eta(t) \rangle = 0$ and $\langle \eta(t) \eta(t') \rangle = d \delta(t - t')$.

In Fig. 2, the phase portrait of the concentrations of X_n and Y_n is shown for $n = 1, 15, 30$, when weak noise exists in the concentration of the input chemical species A. Here, the mean concentrations of A and B are $a = 1$ and $b = 1$, respectively. Thus, since the stability condition is satisfied, if no disturbances exist, the concentrations of X_n and Y_n eventually approach the fixed point. However, the small amplitude noise in the concentration of A is being amplified in the downstream reactions (Fig. 2, $n = 15$) and chemical oscillations develop in the further downstream reactions (Fig. 2, $n = 30$). In this way, the system is convectively unstable, and the chemical oscillation in the downstream reactions is noise sustained.

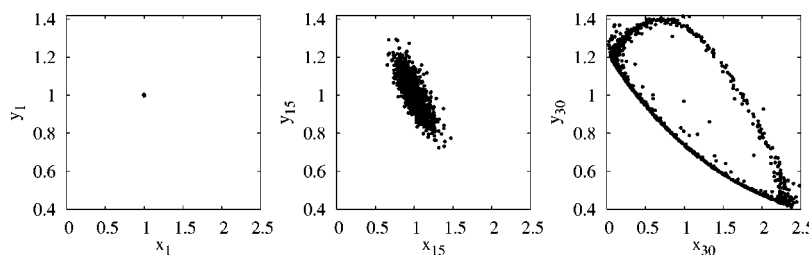


FIG. 2. The phase portrait of the concentration of (X_1, Y_1) , (X_{15}, Y_{15}) , and (X_{30}, Y_{30}) . The values of the parameters are given by $a = 1.0$ and $b = 1.0$.

III. CO-MOVING LYAPUNOV EXPONENT AND PHASE DIAGRAM

This convective instability can be characterized by the co-moving Lyapunov exponents $\lambda(v)$, which describes the exponential growth rate of small amplitude disturbances in a frame moving to the downstream reactions with velocity v [4]. The co-moving Lyapunov exponent has been introduced for the characterization of convective instability in spatially extended systems [4]. Let $(\delta x_1(0), \delta y_1(0))$ be the infinitesimal displacement at the first reaction step at the initial time 0 around the fixed point value, and $(\delta x_{[vt]}(t), \delta y_{[vt]}(t))$ represent the displacement at the $[vt]$ -th reaction step at time t . Here, $[vt]$ gives the integer part of vt . Then, $\lambda(v)$ is given by

$$\lambda(v) = \lim_{t \rightarrow \infty} \frac{1}{t} \log \frac{|(\delta x_{[vt]}(t), \delta y_{[vt]}(t))|}{|(\delta x_1(0), \delta y_1(0))|}. \tag{5}$$

The co-moving Lyapunov exponent for the velocity $v=0$ is the maximum Lyapunov exponent. If $\lambda(0)$ is negative and the $\lambda(v)$ is positive for some v , then the system is convectively unstable. If $\lambda(v) < 0$ for any v , then the system is absolutely stable. If $\lambda(0) > 0$, then the system is absolutely unstable.

Figure 3 shows the co-moving Lyapunov exponent about the fixed point calculated numerically and plotted as a function of v . $\lambda(0)$ is the Lyapunov exponent of the single Brusselator at the fixed point. As the velocity v increases, $\lambda(v)$ becomes larger than zero and is a concave function of v .

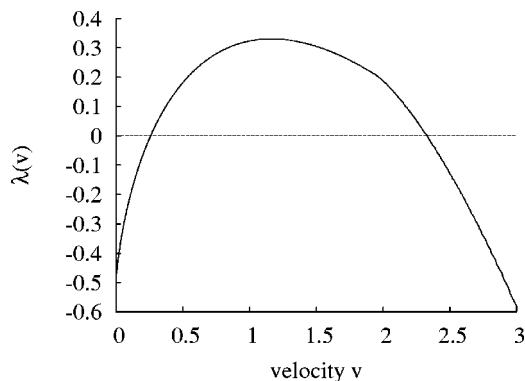


FIG. 3. The co-moving Lyapunov exponent calculated numerically and plotted as a function of velocity v . The parameter values are given by $a = 1.0$ and $b = 1.0$.

Therefore, this cascade chemical reaction system shows the typical property of convectively unstable systems.

Figure 4 gives the phase diagram determined numerically. The parameter points of convectively unstable and absolutely stable phases are plotted according to the co-moving Lyapunov exponent analysis. The convective instability is observed in a wide parameter region between the absolutely stable and absolutely unstable regions.

IV. AMPLIFICATION EXPONENT PER REACTION STEP

As shown in Fig. 2, weak noise added to the first reaction is amplified in the downstream reactions. It is interesting to study how the small amplitude noise in the input chemical A affects the behavior of the downstream chemical species. The typical amplitude at the n th step reaction is given by $O(\delta x_n, \delta y_n) \sim \sqrt{d} e^{\gamma n}$, where γ is the amplification exponent per reaction step, which characterizes the exponential growth of the amplitude as the reaction step n increases. Since $\lambda(v)$ is the growth rate for the velocity v , the growth rate per reaction step is given by $\lambda(v)/v$ [8,9]. For large n , we have

$$\gamma = \max_v \lambda(v)/v. \tag{6}$$

The growth rate γ has been called the ‘‘spatial Lyapunov exponent’’ in spatially extended systems [8,9]. The present

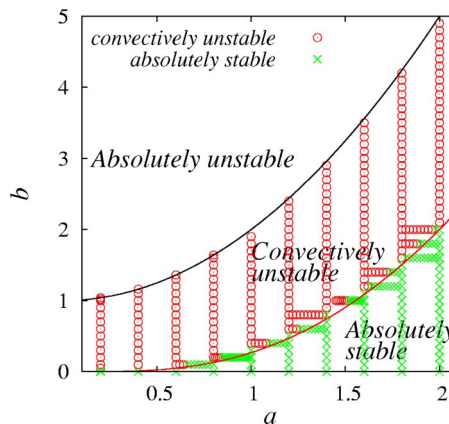


FIG. 4. The phase diagram. The parameter points where the maximum co-moving Lyapunov exponent is negative are shown by crosses, whereas the parameter points where the maximum co-moving Lyapunov exponent is positive are displayed by circles. The line $b = a^2 + 1$ indicates the Hopf bifurcation line and the line $b = a^2 + 1 - \sqrt{2a^2 + 1}$ indicates the bifurcation of convective instability.

system has, however, no spatial coordinate. Therefore, in this paper we call γ the amplification exponent. Notice that Eq. (6) is correct only for the nonintermittent case [10]. In general, the right-hand side of Eq. (6) gives a lower bound of γ .

The amplification exponent γ can be calculated explicitly by studying the linearized evolution equation. To do this, the Fourier representation of the linearized evolution equation is useful. The Fourier method has been applied for linearized evolution equation of open flow systems [14–16]. Here, it is shown that this analysis can be applied to obtain the amplification exponent or the spatial Lyapunov exponent for spatial extended systems.

Let ξ_n and ψ_n be small deviations about the steady—state concentrations of x_n and y_n , respectively. Then, the linear evolution equations for $\xi_n(t)$ and $\psi_n(t)$ around the fixed point of (x_n, y_n) are given by

$$\begin{pmatrix} \dot{\xi}_n \\ \dot{\psi}_n \end{pmatrix} = A \begin{pmatrix} \xi_n \\ \psi_n \end{pmatrix} + \begin{pmatrix} 1 & 0 \\ 0 & 0 \end{pmatrix} \begin{pmatrix} \xi_{n-1} \\ \psi_{n-1} \end{pmatrix}, \quad (7)$$

where A is a matrix given by

$$A = \begin{pmatrix} b-1 & a^2 \\ -b & -a^2 \end{pmatrix}. \quad (8)$$

The Fourier series expansions of $\xi_n(t)$ and $\psi_n(t)$ in the interval $[0, T]$ are given by

$$\xi_n(t) = \sum_{k=-\infty}^{\infty} \Xi_n(k) e^{i\omega_k t}, \quad (9)$$

$$\psi_n(t) = \sum_{k=-\infty}^{\infty} \Psi_n(k) e^{i\omega_k t}, \quad (10)$$

where the frequency ω_k is

$$\omega_k = \frac{2\pi k}{T} \quad (k=0, \pm 1, \pm 2, \dots). \quad (11)$$

The Fourier coefficients Ξ_n and Ψ_n are

$$\Xi_n(k) = \frac{1}{T} \int_0^T \xi_n(t) e^{-i\omega_k t} dt \quad (12)$$

and

$$\Psi_n(k) = \frac{1}{T} \int_0^T \psi_n(t) e^{-i\omega_k t} dt. \quad (13)$$

Then, Eq. (7) leads to

$$(i\omega_n E - A) \begin{pmatrix} \Xi_n(k) \\ \Psi_n(k) \end{pmatrix} = \begin{pmatrix} 1 & 0 \\ 0 & 0 \end{pmatrix} \begin{pmatrix} \Xi_{n-1}(k) \\ \Psi_{n-1}(k) \end{pmatrix}, \quad (14)$$

where E is the identity matrix. Thus, $\Xi_n(k)$ is obtained as

$$\Xi_n(k) = \mathcal{F}(\omega_k) \Xi_{n-1}(k) \quad (15)$$

with transfer function $\mathcal{F}(\omega)$,

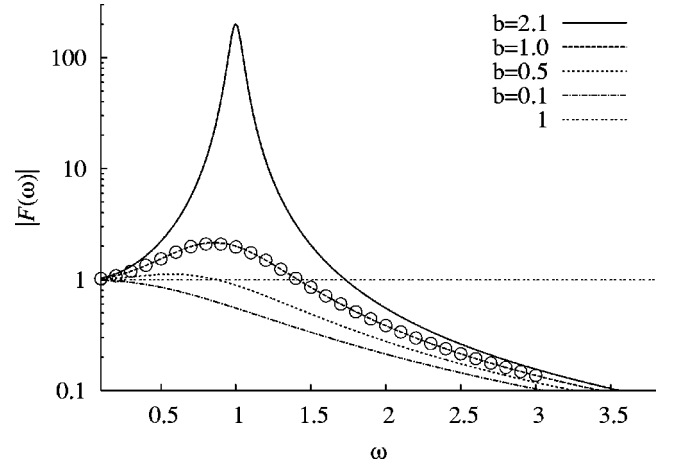


FIG. 5. The transfer function $\mathcal{F}(\omega)$ plotted as $|\mathcal{F}(\omega)|$ for $a=1$ and $b=2.1, 1.0, 0.5$ and 0.1 . The amplification exponent per reaction step $\gamma_n(\omega)$ obtained by solving Eq. (3) with Eq. (29) for $b=1$ is also plotted as $\exp[2.0\gamma_n(\omega)]$ (\circ). Here, we choose $n=10$.

$$\mathcal{F}(\omega) = (1, 0)(i\omega E - A)^{-1} \begin{pmatrix} 1 \\ 0 \end{pmatrix} \quad (16)$$

$$= \frac{i\omega + a^2}{-\omega^2 + (a^2 - b + 1)i\omega + a^2}. \quad (17)$$

In order to find the amplification exponent per reaction step, suppose that the white Gaussian noise is added at the top of the cascade, and study the response of the downstream chemical species. For this, suppose $x_0(t) = a + \eta(t)$ in Eq. (3), where $\eta(t)$ is the white Gaussian noise with $\langle \eta(t) \rangle = 0$ and $\langle \eta(t)\eta(t') \rangle = d\delta(t-t')$. Then, the power spectrum density of $\eta(t)$ is given by

$$P_0(\omega) = \lim_{T \rightarrow \infty} \frac{T}{2\pi} \langle |\Xi_0(n)|^2 \rangle = \frac{d}{2\pi}. \quad (18)$$

The power spectrum density of $\xi_n(t)$ for the n th chemical species is given by

$$P_n(\omega) = \lim_{T \rightarrow \infty} \frac{T}{2\pi} \langle |\Xi_n(k)|^2 \rangle. \quad (19)$$

Substituting Eqs. (15) and (18) into this, it follows that

$$P_n(\omega) = |\mathcal{F}(\omega)|^{2n} \frac{d}{2\pi}. \quad (20)$$

In the present case, $|\mathcal{F}(\omega)|$ is given by

$$|\mathcal{F}(\omega)|^2 = \frac{a^4 + \omega^2}{(a^2 - \omega^2)^2 + \omega^2(a^2 - b + 1)^2}. \quad (21)$$

If $|\mathcal{F}(\omega)|$ is smaller than unity for any ω , the small disturbances damped out at the downstream reactions. On the other hand, if $|\mathcal{F}(\omega)|$ is larger than unity for some ω , it is expected that the small disturbance grows as the reaction step increases. In Fig. 5, $|\mathcal{F}(\omega)|$ is plotted as a function of ω (lines), showing that $|\mathcal{F}(\omega)|$ becomes larger than unity for

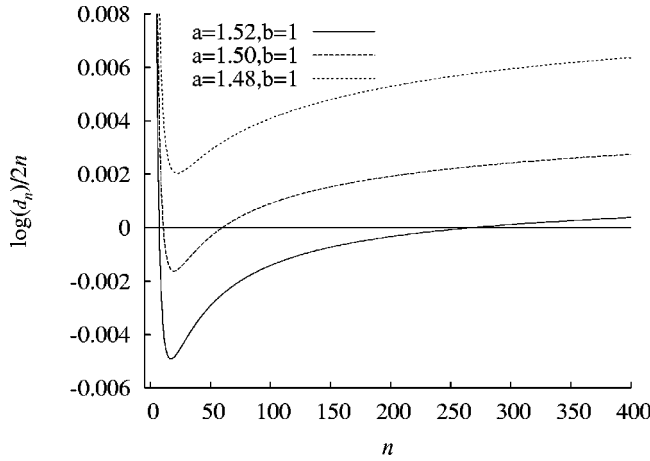


FIG. 6. The amplification exponent $\gamma_n = \log d_n/d/2n$ plotted as functions of reaction step n .

some values of ω depending on the parameter value.

Now we calculate the amplification exponent per reaction step. Let γ_n give the amplification exponent at the n th step [17], which is defined as

$$\gamma_n = \frac{1}{2n} \log(d_n/d), \quad (22)$$

in which d_n is the dispersion of $\xi_n(t)$, which is obtained by

$$d_n = \langle \xi_n(t)\xi_n(t) \rangle = \int_{-\infty}^{\infty} P_n(\omega) d\omega. \quad (23)$$

Thus, the amplification rate γ_n is calculated by substituting Eqs. (20) and (23) into Eq. (22). Then we have

$$\gamma_n = \frac{1}{2n} \log \int_{-\infty}^{\infty} |F(\omega)|^{2n} d\omega - \frac{1}{2n} \log 2\pi. \quad (24)$$

In Fig. 6, the amplification exponent γ_n is plotted as a function of n . For the calculation of γ_n , substituting Eq. (21) into Eq. (24), we adopted a numerical integration method. The amplification exponent γ_n approaches to a particular value as n increases. For sufficiently large n , the maximum value of $|F(\omega)|$ dominates the amplification. Thus, the amplification exponent approaches

$$\gamma = \lim_{n \rightarrow \infty} \gamma_n = \log(|F(\omega^*)|)/2, \quad (25)$$

where

$$|F(\omega^*)| = \max_{\omega} |F(\omega)|. \quad (26)$$

In the present case, ω^* is calculated at

$$(\omega^*)^2 = -a^4 + a^2 \sqrt{2a^2b + 2b - b^2}. \quad (27)$$

In this way, the amplification exponent is obtained by substituting Eq. (21) into Eq. (25) with this ω^* .

In Fig. 7, the amplification exponent per reaction step γ given by Eq. (25) is plotted as a function of a (solid line). The amplification exponent is also obtained numerically by

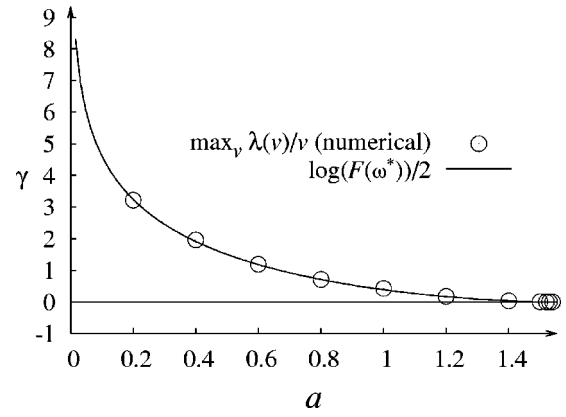


FIG. 7. The amplification exponent per one step reaction plotted as a function of a . The growth rates per one step obtained from the co-moving Lyapunov exponent are shown by circles. The growth rate given by $\gamma = \log(|F(\omega^*)|)/2$ is displayed by a solid line. The parameter value is given by $b=1.0$.

applying Eq. (6) to the co-moving Lyapunov exponent. In order to compare the amplification exponents obtained in such ways, both of them are plotted in Fig. 7, showing good agreement with each other. Thus, the present analysis yields the amplification exponent per reaction step or the spatial Lyapunov exponent for spatial extended systems.

According to this analysis, the system is convectively unstable if $|F(\omega^*)|$ is larger than unity. This condition gives the bifurcation points of the convective instability. In the present case, $|F(\omega^*)| > 1$ if the inequality

$$b > a^2 + 1 - \sqrt{2a^2 + 1} \quad (28)$$

is satisfied. The bifurcation line given by Eq. (28) is plotted in the phase diagram in Fig. 4. The bifurcation line obtained in this analysis is in good agreement with the bifurcation line obtained numerically according to the co-moving Lyapunov exponent analysis.

Before concluding this section, we should note the following two points. The amplification exponent γ_n can be negative for some small n , even when the system is convectively unstable. Thus, the induction steps, where the amplitude growth to $O(1)$, cannot be obtained in a straightforward way. The second point is that $|F(\omega)|$ can give the frequency-dependent amplification exponent. We shall study this frequency dependence in the next section.

V. MODULATION OF THE INLET CHEMICAL CONCENTRATION

The effect of the boundary modulation on flow systems has been studied theoretically and experimentally [2,6]. The studies have shown that attractors can be selected by controlling the frequency of boundary modulation. In the present analysis, the transfer function $F(\omega)$, shown in Fig. 5, implies the amplification exponent that depends on the frequency of modulation of the input chemical concentration. Thus, such a frequency-dependent amplification exponent could provide some information on the effects of the boundary modulation.

A. Frequency dependent amplification exponent

Let us investigate the situation where the concentration of chemical species A is oscillating in time with frequency ω . Therefore, we consider the evolution equation Eq. (3) with

$$x_0(t) = a + \delta \sin(\omega t), \quad (29)$$

where δ is the amplitude of modulation and ω is its frequency.

The behavior of the downstream reactions could depend on the values of δ and ω . Here, we only study the case where δ takes a small value, in order to pay attention to the frequency dependence of pattern dynamics. Therefore, hereafter we fix the value of δ to be 0.01.

First we study the amplification exponent of small amplitude modulation numerically by solving the evolution equation Eq. (3) with Eq. (29) [18]. In order to measure the amplification exponent, the mean square deviation $\langle \delta x_n^2 \rangle = \langle x_n^2 \rangle - \langle x_n \rangle^2$ is calculated for X_n . Here, $\langle \cdot \rangle$ means temporal average over a sufficiently long time interval. Then, the amplification exponent is given by [17]

$$\gamma_n(\omega) = \frac{1}{n} \log \left(\frac{\langle \delta x_n^2 \rangle}{\langle \delta x_0^2 \rangle} \right). \quad (30)$$

In Fig. 5, for comparing the amplification exponent obtained numerically with the transfer function $|\mathcal{F}(\omega)|$, $\exp[2.0\gamma_n(\omega)]$ is plotted as a function of the frequency ω for sufficiently large n (here $n=120$). The frequency-dependent amplification exponent obtained numerically is in good agreement with the transfer function. Hence, the transfer function $\mathcal{F}(\omega)$ gives the frequency dependence of the amplification exponent per reaction step or the spatial Lyapunov exponent for spatially extended systems.

B. Selection of oscillation in the downstream reactions

As the reaction step increases, the amplitude of the chemical oscillation grows and reaches saturation due to the nonlinearity. For the frequency of the oscillation at the downstream reactions a particular value is selected. This nonlinear evolution of chemical oscillation depends strongly on the frequency of the oscillation in the inlet chemical concentration. In Fig. 8, the frequency selected at the downstream reactions is plotted as a function of the modulation frequency in the inlet chemical concentration. In Fig. 9, the amplitude saturated at the downstream reactions is plotted as a function of the frequency of the oscillation selected in the downstream reactions, indicating the almost one-to-one correspondence between them.

The selected frequency shown in Fig. 8 is one of the harmonic components of the modulation frequency ω of the inlet chemical concentration. It may be interesting to ask what determines the frequency of the oscillation selected at the downstream reactions. Here, we only note that the frequency-dependent amplification exponent does not determine the frequency selected in the downstream reactions. In other words, even if $|F(\ell\omega)| > |F(m\omega)|$, ($\ell \neq m, \ell, m = 1, 2, 3, \dots$), this does not necessarily mean that the frequency $\ell\omega$ will be selected.

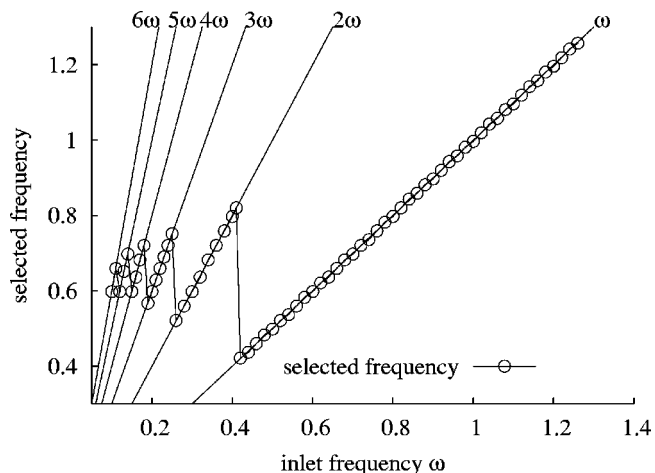


FIG. 8. The amplitude saturated in the downstream reactions plotted as a function of ω , which is the modulation frequency of the concentration of inlet chemical species A. As the amplitude, mean square deviation of x_n at $n=120$ is adopted. The parameter values are $a=1.0$ and $b=1.0$.

VI. CONCLUSION

In this paper, we have studied a cascade chemical reaction, which consists of a series of unidirectionally coupled Brusselators. It has been shown that the small disturbances are amplified along the cascade and the noise-sustained chemical oscillation is developed in the downstream reactions. This is the typical properties of open flow systems, called *convective instability*. The co-moving Lyapunov exponent and the amplification exponent per reaction step (spatial Lyapunov exponent) are the characterizations of the convective instability. In the present paper, we have focused on the amplification exponent per reaction step (the spatial Lyapunov exponent). The exponent obtained analytically is shown to be in good agreement with that obtained numerically from the co-moving Lyapunov exponent. Therefore, a

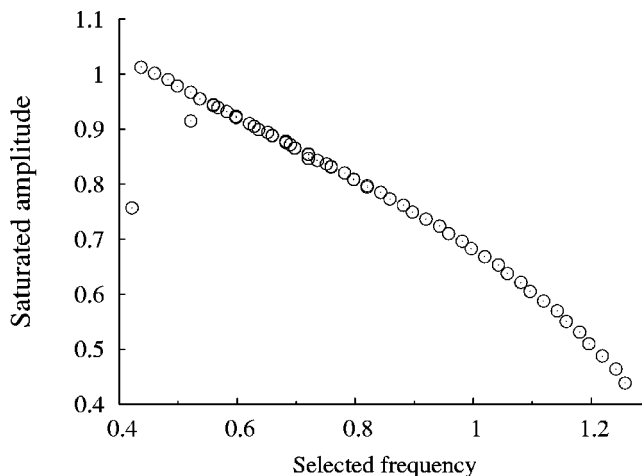


FIG. 9. The saturated amplitude plotted as a function of the selected frequency of the chemical oscillation. The parameter values are $a=1.0, b=1.0$. The amplitude is measured at $n=120$.

relationship between the analysis based on the co-moving Lyapunov exponent and the present analysis based on the Fourier method is clearly elucidated. We have finally studied the amplification of the modulation in the inlet chemical concentration. The amplification rate is determined by the frequency-dependent amplification exponent, which, however, does not determine the oscillation selected in the downstream reactions.

In the present study, we supposed that the system can be described by a *macroscopic* equation. This means that the stochastic fluctuation in the evolution of the concentrations is neglected. Then, the noise added externally at the inlet

chemical concentration sustains the formation of oscillation in the downstream reactions. However, intrinsic noise existing in chemical reactions could also lead to the formation of patterns. In particular, the possibility of the noise-sustained formation of patterns in small reaction systems such as cells remains to be clarified.

The author is grateful to K. Fujimoto and S. Ishihara for stimulating discussions and to A. S. Mikhailov for critical reading of this manuscript. The author gratefully acknowledges the support from the Alexander von Humboldt Foundation (Germany).

-
- [1] R. J. Deisler, *Physica D* **25** 233 (1987).
 [2] J. Liu and J. P. Gollub, *Phys. Rev. Lett.* **70**, 2289 (1993).
 [3] K. Otsuka and K. Ikeda, *Phys. Rev. A* **39**, 5209 (1989).
 [4] R. J. Deisler and K. Kaneko, *Phys. Lett. A* **119**, 397 (1987).
 [5] J. P. Crutchfield and K. Kaneko, *Directions in Chaos* (World Scientific, Singapore, 1987), Vol 1.
 [6] F. H. Willeboordse and K. Kaneko, *Physica D* **86**, 428 (1995).
 [7] T. Bohr and D. A. Rand, *Physica D* **52**, 532 (1991).
 [8] D. Vergni, M. Falcioni, and A. Vulpiani, *Phys. Rev. E* **56**, 6170 (1997).
 [9] A. Politi and A. Torcini, *Chaos* **2**, 293 (1992).
 [10] G. Boffetta, M. Cencini, M. Falcioni, and A. Vulpiani, *Phys. Rep.* **356**, 367 (2002).
 [11] K. Fujimoto and K. Kaneko, *Physica D* **129**, 203 (1999).
 [12] M. Samoilov, A. Arkin, and J. Ross, *J. Phys. Chem. A* **106**, 10205 (2002).
 [13] R. E. Dolmetsch, K. Xu and R. S. Lewis, *Nature (London)* **392**, 933 (1998); W. Li, J. Llopis, M. Whitney, G. Zlokarnik, and R. Y. Tsien, *Nature (London)* **392**, 936 (1998).
 [14] O. Rudzick and A. Pikovsky, *Phys. Rev. E* **54**, 5107 (1996).
 [15] K. Konishi, H. Kokame, and K. Hirata, *Phys. Rev. E* **62**, 6383 (2000).
 [16] K. Konishi, *Phys. Rev. E* **65**, 036203 (2002).
 [17] Note that γ_n in Eq. (22) and $\gamma_n(\omega)$ in Eq. (30) are considered as a kind of generalized Lyapunov exponent. See Ref. [10].
 [18] Calculating Eq. (3) with Eq. (29) numerically, round-off errors also grow exponentially along the cascade. Thus, we used the Runge-Kutta method with quadruple precision real numbers in order to calculate the sufficiently large cascade. Here, the size of the cascade is $n=120$.